Front. Optoelectron. China 2010, 3(3): 292–302
DOI 10.1007/s12200-010-0111-z

RESEARCH ARTICLE

Diffraction of Lorentz-Gauss beam in uniaxial crystals: orthogonal to optical axis

Jia LI (✉), Yanru CHEN, Shixue XU, Yongqing WANG, Muchun ZHOU, Qi ZHAO, Yu XIN, Feinan CHEN

Department of Optical Engineering, Nanjing University of Science and Technology, Nanjing 210094, China

© Higher Education Press and Springer-Verlag Berlin Heidelberg 2010

Abstract Based on the diffraction theory of beams in uniaxial crystals, diffraction properties of a Lorentz-Gauss beam in uniaxial crystals orthogonal to the optical axis are derived in analytical forms. Diffraction fields, intensity distributions and effects of beam parameters are investigated by numerical examples, respectively. Results show that, upon propagation, initial field components and intensity distributions of Lorentz-Gauss beams would deteriorate due to effects of anisotropic media. When the Lorentz-Gauss beam diffracts into the far field, its intensity distribution would convert into a four-petal profile. Beam parameters w_x and w_y are shown to have a strong influence on intensity distributions. By selecting different values of them, profiles of Lorentz-Gauss beams would be different upon propagation.

Keywords Lorentz-Gauss beam, uniaxial crystal, intensity distribution, anisotropic media

1 Introduction

In recent years, diode lasers have been widely used as the light source in practical applications, such as fiber communications, optical sensors, optical measurement instruments, etc. Among these applications, some literatures describe analytical expressions for the far field of the emitted light of diode lasers, based on Maxwell's equations [1–3]. For example, a simple Gaussian model of diode laser beams has been proposed and widely used in coupling systems between a diode and an optical fiber [4]. Very recently, a new realizable beam type named the Lorentz-Gauss beam has been introduced [5,6]. Compared to the Gaussian distribution, the Lorentz-Gaussian distribution occupies higher angular spreading characteristics, which provides a more appropriate model to describe the radiation emitted by a single mode diode laser [3]. Also it has been confirmed that the Lorentz-Gaussian beam is valid to describe a variety of commercially available double heterojunction $Ga_{1-x}Al_xAs$ lasers, whose active regions are as narrow as 0.1 μm for a typical emission wavelength of 0.8 μm [2]. Therefore, relatively highly divergent optical fields are realizable in the far field of this beam. As a result, the Lorentz-Gauss beam provides a more appropriate model to describe some non-paraxial laser beams [7,8]. So far many investigations have been carried out by researchers concerning propagation properties of Lorentz-Gauss beams in/through various media [9–13].

On the other hand, presently anisotropic media has become a hot subject both in theoretical and experimental aspects because it plays an essential role in designing polarizers and compensators, etc. [14]. Because of its importance in practical applications, in past years, researchers have studied the propagation of various laser beams in uniaxial crystals by solving Maxwell's equations, in cases of beams propagating orthogonal to the optical axis [15–21] and along the optical axis [22–27]. The works referred above are invaluable and significant; however, to the best of our knowledge, there has been no report on diffraction properties of the Lorentz-Gauss beam in anisotropic media, so it is essential to know its exact diffraction field in uniaxial crystals.

To solve the issue stated above, in this paper, diffraction properties of Lorentz-Gauss beams in uniaxial crystals orthogonal to the optical axis are derived in analytical forms, and some numerical examples are illustrated to show their behaviors upon propagation. Effects of beam parameters on propagation properties in uniaxial crystals are also illustrated and further discussed. Results show that, upon propagation in uniaxial crystals, Lorentz-Gauss beams lose their symmetric distributions and show different spreading speed in x and y directions, which is induced by the effect of anisotropic refractive media. It

Received April 13, 2010; accepted May 11, 2010

E-mail: lijiafeifei@sina.com

also shows that, when the Lorentz-Gauss beam diffracts into the far field, its intensity distribution would convert into a four-petal profile. By selecting a different beam waist width of Lorentz parts in the source plane, intensity distributions would be different upon propagation.

2 Theory analysis

It is assumed that a Lorentz-Gauss beam is incident on uniaxial crystals at the initial plane $z = 0$ and propagates along the z axis. The optical axis of the crystal coincides with the x-axis of the Cartesian coordinate system, which is orthogonal to the propagation axis. In this paper, the evanescent field component is negligible so it can be omitted. The dielectric tensor of the crystal can be written as [15–21]

$$\varepsilon = \begin{pmatrix} n_{\mathrm{e}}^2 & 0 & 0 \\ 0 & n_{\mathrm{o}}^2 & 0 \\ 0 & 0 & n_{\mathrm{o}}^2 \end{pmatrix}, \tag{1}$$

where n_{e}, n_{o} being the refractive indices of the extra-ordinary and ordinary light, respectively.

Assuming that a Lorentz-Gauss beam in the initial plane $z = 0$ is linearly polarized along the x-axis, and its analytical expression takes the following form [8–12]:

$$E(x,y;0) = \frac{1}{w_x w_y[1+(x^2/w_x^2)][1+(y^2/w_y^2)]} \cdot \exp\left(-\frac{x^2+y^2}{w_0^2}\right)\boldsymbol{e}_x, \tag{2}$$

where w_0 is the waist width of the Gaussian part; w_x, w_y are the beam parameters related to the width of Lorentz parts in x and y directions, respectively. In this paper the time variant factor $\exp(-\mathrm{i}\omega t)$ is omitted in Eq. (2). Recalling the relationship between the Lorentz function and the orthogonal Hermite-Gaussian function [12,28]:

$$\frac{1}{j^2+w_j^2} = \frac{\sqrt{\pi}}{\sqrt{2}w_j^2}\sum_{m=0}^{N} a_{2m} H_{2m}\left(\frac{j}{w_j}\right)\exp\left(-\frac{j^2}{2w_j^2}\right), \quad j = x,y, \tag{3}$$

where N is the expanded number, a_{2m} is the weight coefficient which can be indexed in Ref. [28]. $H_{2m}(\cdot)$ is the Hermite polynomial of the order $2m$. Substituting Eq. (3) into Eq. (2), the boundary electric field in the initial plane becomes

$$E(x,y;0) = \frac{\pi}{2w_x w_y}\sum_{m=0}^{N}\sum_{n=0}^{N} a_{2m} b_{2n} H_{2m}\left(\frac{x}{w_x}\right) H_{2n}\left(\frac{y}{w_y}\right) \cdot \exp\left(-\frac{x^2}{f_x^2}-\frac{y^2}{f_y^2}\right)\boldsymbol{e}_x, \tag{4}$$

where f_x, f_y are given by

$$\frac{1}{f_j^2} = \frac{1}{w_0^2} + \frac{1}{2w_j^2}, \quad j = x,y. \tag{5}$$

According to the diffraction theory of beams in uniaxial crystals orthogonal to the optical axis, the electric field of a beam after propagating a distance z in uniaxial crystals can be expressed as [15–21]

$$\begin{aligned} E(p,q;z) &= \int \mathrm{d}k_x \mathrm{d}k_y \exp(\mathrm{i}k_x p + \mathrm{i}k_y q)\exp(\mathrm{i}k_{\mathrm{e}z} z) \\ &\times \begin{pmatrix} \tilde{E}_x(k_x,k_y;0) \\ -\dfrac{k_x k_y}{k_0^2 n_{\mathrm{o}}^2 - k_x^2}\tilde{E}_x(k_x,k_y;0) \\ -\dfrac{k_{\mathrm{e}z} k_x}{k_0^2 n_{\mathrm{o}}^2 - k_x^2}\tilde{E}_x(k_x,k_y;0) \end{pmatrix} \\ &+ \int \mathrm{d}k_x \mathrm{d}k_y \exp(\mathrm{i}k_x p + \mathrm{i}k_y q)\exp(\mathrm{i}k_{\mathrm{o}z} z) \\ &\times \begin{pmatrix} 0 \\ \dfrac{k_x k_y}{k_0^2 n_{\mathrm{o}}^2 - k_x^2}\tilde{E}_x(k_x,k_y;0) + \tilde{E}_y(k_x,k_y;0) \\ -\dfrac{k_y}{k_{0z}}\left[\dfrac{k_x k_y}{k_0^2 n_{\mathrm{o}}^2 - k_x^2}\tilde{E}_x(k_x,k_y;0) + \tilde{E}_y(k_x,k_y;0)\right] \end{pmatrix}, \end{aligned} \tag{6}$$

where p and q are transversal positions in the output plane z, k_0 is the wave number related with the wavelength as $k_0 = 2\pi/\lambda$. $\tilde{E}_j$ is the two-dimensional Fourier transform of the electric field component in the plane $z = 0$, which is given by

$$\tilde{E}_j(k_x,k_y;0) = \frac{1}{(2\pi)^2}\int \mathrm{d}x\mathrm{d}y \exp(-\mathrm{i}k_x x - \mathrm{i}k_y y)E_j(x,y;0), \quad j = x,y. \tag{7}$$

$k_{\mathrm{o}z}$ and $k_{\mathrm{e}z}$ shown in Eq. (6) are represented by

$$k_{\mathrm{o}z}(k_x,k_y) = \sqrt{k_0^2 n_{\mathrm{o}}^2 - k_x^2 - k_y^2}, \tag{8a}$$

$$k_{\mathrm{e}z}(k_x,k_y) = \sqrt{k_0^2 n_{\mathrm{e}}^2 - (n_{\mathrm{e}}^2/n_{\mathrm{o}}^2)k_x^2 - k_y^2}. \tag{8b}$$

Equation (6) gives the exact solutions to the electric field of electromagnetic beams through uniaxial crystals orthogonal to the optical axis. Because of the fact that generally the Lorentz-Gauss beam is generated by the

double heterojunction $Ga_{1-x}Al_xAs$ laser resonators, it would have high divergence in the far field. In this case the non-paraxial propagation of Lorentz-Gauss beams in uniaxial crystals must be considered. However, the integral format in Eq. (6) cannot be further performed for non-paraxial diffraction of Lorentz-Gaussian beams. In this paper, it is assumed that the paraxial propagation case (Eq. (15) of Ref. [15]) is applied for the Lorentz-Gaussian beam diffracting in uniaxial crystals. Therefore, relations $k_x \ll k_0$, $k_y \ll k_0$ are satisfied and the factors k_{oz} and k_{ez} in Eq. (6) can be truncated by Taylor expansions in k_x/k_0 and k_y/k_0 for the phases and amplitudes up to the second order [15]. After some algebraic operations Eq. (6) can be arranged into

$$\begin{aligned} E_{ex}(p,q;z) &= \exp(ik_0 n_e z)\cdot A_{ex}(p,q;z) \\ &= \exp(ik_0 n_e z)\times\int dk_x dk_y \exp\left(ik_x p + ik_y q - i\frac{n_e^2 k_x^2 + n_o^2 k_y^2}{2k_0 n_o^2 n_e} z\right)\tilde{E}_x(k_x,k_y;0), \end{aligned} \tag{9a}$$

$$\begin{aligned} E_{ey}(p,q;z) &= \exp(ik_0 n_e z)\cdot A_{ey}(p,q;z) \\ &= \exp(ik_0 n_e z)\times\int dk_x dk_y \exp\left(ik_x p + ik_y q - i\frac{n_e^2 k_x^2 + n_o^2 k_y^2}{2k_0 n_o^2 n_e} z\right)\left(-\frac{k_x k_y}{k_0^2 n_o^2}\right)\tilde{E}_x(k_x,k_y;0), \end{aligned} \tag{9b}$$

$$\begin{aligned} E_{ez}(p,q;z) &= \exp(ik_0 n_e z)\cdot A_{ez}(p,q;z) \\ &= \exp(ik_0 n_e z)\times\int dk_x dk_y \exp\left(ik_x p + ik_y q - i\frac{n_e^2 k_x^2 + n_o^2 k_y^2}{2k_0 n_o^2 n_e} z\right)\left(-\frac{n_e k_x}{k_0 n_o^2}\right)\tilde{E}_x(k_x,k_y;0), \end{aligned} \tag{9c}$$

$$E_{ox}(p,q;z) = 0, \tag{9d}$$

$$\begin{aligned} E_{oy}(p,q;z) &= \exp(ik_0 n_o z)\cdot A_{oy}(p,q;z) \\ &= \exp(ik_0 n_o z)\times\int dk_x dk_y \exp\left(ik_x p + ik_y q - i\frac{k_x^2 + k_y^2}{2k_0 n_o} z\right)\times\left(\frac{k_x k_y}{k_0^2 n_o^2}\tilde{E}_x(k_x,k_y;0) + \tilde{E}_y(k_x,k_y;0)\right), \end{aligned} \tag{9e}$$

$$\begin{aligned} E_{oz}(p,q;z) &= \exp(ik_0 n_o z)\cdot A_{oz}(p,q;z) \\ &= \exp(ik_0 n_o z)\times\int dk_x dk_y \exp\left(ik_x p + ik_y q - i\frac{k_x^2 + k_y^2}{2k_0 n_o} z\right)\left(-\frac{k_y}{k_0 n_o}\right)\tilde{E}_y(k_x,k_y;0). \end{aligned} \tag{9f}$$

Substituting Eq. (4) into Eq. (7), the two-dimensional Fourier transform of the electric field in the initial plane $z = 0$ is obtained:

$$\tilde{E}_x(k_x,k_y;0) = \frac{f_x f_y}{8 w_x w_y}\sum_{m=0}^{N}\sum_{n=0}^{N} a_{2m} b_{2n} H_{2m}(w_x k_x) H_{2n}(w_y k_y)\exp\left(-\frac{f_x^2}{4}k_x^2 - \frac{f_y^2}{4}k_y^2\right), \tag{10a}$$

$$\tilde{E}_y(k_x,k_y;0) = 0. \tag{10b}$$

Substituting Eq. (10) into Eq. (9) and recalling the two following formulas [29]:

$$(k_j)^n \exp(ik_j\cdot j) = \left(-i\frac{\partial}{\partial j}\right)^n \exp(ik_j\cdot j), \quad j = x,y, \tag{11}$$

$$\int_{-\infty}^{+\infty}\exp\left(-\frac{\gamma^2}{2}\right)H_s(\gamma)\exp(i\gamma\xi) = (2\pi)^{1/2}\exp\left(-\frac{\xi^2}{2}\right)H_s(\xi)\cdot i^s, \tag{12}$$

after tedious but straightforward integrations, amplitudes of the electric field in the reference plane z can be obtained:

$$\begin{aligned}A_{\mathrm{ex}}(p,q;z)=&\frac{\pi f_x f_y}{2w_x w_y}\frac{1}{Q_x}\frac{1}{Q_y}\exp\left(-\frac{p^2}{Q_x^2}-\frac{q^2}{Q_y^2}\right)\\&\times\sum_{m=0}^{N}a_{2m}\left(1-\frac{4w_x^2}{Q_x^2}\right)^m H_{2m}\left(\frac{1}{2}\mathrm{i}w_x p\Big/\sqrt{\left(\frac{Q_x^2}{4}\right)^2-\frac{Q_x^2}{4}w_x^2}\right)\\&\times\sum_{n=0}^{N}b_{2m}\left(1-\frac{4w_y^2}{Q_y^2}\right)^n H_{2n}\left(\frac{1}{2}\mathrm{i}w_y q\Big/\sqrt{\left(\frac{Q_y^2}{4}\right)^2-\frac{Q_y^2}{4}w_x^2}\right),\end{aligned}\tag{13}$$

$$\begin{aligned}A_{\mathrm{ey}}(p,q;z)=&\frac{1}{k_0^2 n_{\mathrm{o}}^2}\frac{\pi f_x f_y}{2w_x w_y}\frac{1}{Q_x}\frac{1}{Q_y}\sum_{m=0}^{N}a_{2m}\left(1-\frac{4w_x^2}{Q_x^2}\right)^m\\&\times\frac{\partial}{\partial p}\exp\left(-\frac{p^2}{Q_x^2}\right)H_{2m}\left(\frac{1}{2}\mathrm{i}w_x p\Big/\sqrt{\left(\frac{Q_x^2}{4}\right)^2-\frac{Q_x^2}{4}w_x^2}\right)\\&\times\sum_{n=0}^{N}b_{2n}\left(1-\frac{4w_y^2}{Q_y^2}\right)^n\times\frac{\partial}{\partial q}\exp\left(-\frac{q^2}{Q_y^2}\right)\\&\times H_{2n}\left(\frac{1}{2}\mathrm{i}w_y q\Big/\sqrt{\left(\frac{Q_y^2}{4}\right)^2-\frac{Q_y^2}{4}w_y^2}\right),\end{aligned}\tag{14a}$$

$$\begin{aligned}A_{\mathrm{ez}}(p,q;z)=&\frac{\mathrm{i}n_{\mathrm{e}}}{k_0 n_{\mathrm{o}}^2}\frac{\pi f_x f_y}{2w_x w_y}\frac{1}{Q_x}\frac{1}{Q_y}\sum_{m=0}^{N}a_{2m}\left(1-\frac{4w_x^2}{Q_x^2}\right)^m\\&\times\frac{\partial}{\partial p}\exp\left(-\frac{p^2}{Q_x^2}\right)H_{2m}\left(\frac{1}{2}\mathrm{i}w_x p\Big/\sqrt{\left(\frac{Q_x^2}{4}\right)^2-\frac{Q_x^2}{4}w_x^2}\right)\\&\times\sum_{n=0}^{N}b_{2n}\left(1-\frac{4w_y^2}{Q_y^2}\right)^n\exp\left(-\frac{q^2}{Q_y^2}\right)\\&\times H_{2n}\left(\frac{1}{2}\mathrm{i}w_y q\Big/\sqrt{\left(\frac{Q_y^2}{4}\right)^2-\frac{Q_y^2}{4}w_y^2}\right),\end{aligned}\tag{14b}$$

$$\begin{aligned}A_{\mathrm{oy}}(p,q;z)=&-\frac{1}{k_0^2 n_{\mathrm{o}}^2}\frac{\pi f_x f_y}{2w_x w_y}\frac{1}{P_x}\frac{1}{P_y}\sum_{m=0}^{N}a_{2m}\left(1-\frac{4w_x^2}{P_x^2}\right)^m\\&\times\frac{\partial}{\partial p}\exp\left(-\frac{p^2}{P_x^2}\right)H_{2m}\left(\frac{1}{2}\mathrm{i}w_x p\Big/\sqrt{\left(\frac{P_x^2}{4}\right)^2-\frac{P_x^2}{4}w_x^2}\right)\\&\times\sum_{n=0}^{N}b_{2n}\left(1-\frac{4w_y^2}{P_y^2}\right)^n\times\frac{\partial}{\partial q}\exp\left(-\frac{q^2}{P_y^2}\right)\end{aligned}$$

$$\times H_{2n}\left(\frac{1}{2}\mathrm{i}w_y q\Big/\sqrt{\left(\frac{P_y^2}{4}\right)^2-\frac{P_y^2}{4}w_y^2}\right), \tag{14c}$$

where factors Q_x, Q_y, P_x, P_y in Eqs. (13) and (14) are presented by

$$Q_x=\sqrt{f_x^2+\frac{2\mathrm{i}n_\mathrm{e}}{k_0 n_\mathrm{o}^2}z},\ Q_y=\sqrt{f_y^2+\frac{2\mathrm{i}}{k_0 n_\mathrm{e}}z},\ P_x=\sqrt{f_x^2+\frac{2\mathrm{i}z}{k_0 n_\mathrm{o}}},\ P_y=\sqrt{f_y^2+\frac{2\mathrm{i}z}{k_0 n_\mathrm{o}}}. \tag{15}$$

Utilizing the expansion formula of Hermite polynomials [29]

$$H_j(x)=\sum_{k=0}^{j/2}\frac{(-1)^k j!}{k!(j-2k)!}(2x)^{j-2k}, \tag{16}$$

and performing the partial derivative in Eq. (14), it can be further rewritten as

$$\begin{aligned}A_{\mathrm{ey}}(p,q;z)=&\frac{1}{k_0^2 n_\mathrm{o}^2}\frac{\pi f_x f_y}{2w_x w_y}\frac{1}{Q_x}\frac{1}{Q_y}\exp\left(-\frac{p^2}{Q_x^2}\right)\\&\times\exp\left(-\frac{q^2}{Q_y^2}\right)\sum_{m=0}^{N}a_{2m}\left(1-\frac{4w_x^2}{Q_x^2}\right)^m\sum_{s=0}^{m}(-1)^s\frac{(2m)!}{s!(2m-2s)!}\\&\times\left(\mathrm{i}w_x\Big/\sqrt{\left(\frac{Q_x^2}{4}\right)^2-\frac{Q_x^2}{4}w_x^2}\right)^{2m-2s}\left((2m-2s)p^{2m-2s-1}-\frac{2p^{2m-2s+1}}{Q_x^2}\right)\\&\times\sum_{n=0}^{N}b_{2n}\left(1-\frac{4w_y^2}{Q_y^2}\right)^n\sum_{t=0}^{N}(-1)^t\frac{(2n)!}{t!(2n-2t)!}\left(\mathrm{i}w_y\Big/\sqrt{\left(\frac{Q_y^2}{4}\right)^2-\frac{Q_y^2}{4}w_y^2}\right)^{2n-2t}\\&\times\left((2n-2t)q^{2n-2t-1}-\frac{2q^{2n-2t+1}}{Q_y^2}\right),\end{aligned} \tag{17a}$$

$$\begin{aligned}A_{\mathrm{ez}}(p,q;z)=&\frac{\mathrm{i}n_\mathrm{e}}{k_0 n_\mathrm{o}^2}\frac{\pi f_x f_y}{2w_x w_y}\frac{1}{Q_x}\frac{1}{Q_y}\exp\left(-\frac{p^2}{Q_x^2}\right)\\&\times\exp\left(-\frac{q^2}{Q_y^2}\right)\sum_{m=0}^{N}a_{2m}\left(1-\frac{4w_x^2}{Q_x^2}\right)^m\sum_{s=0}^{m}(-1)^s\frac{(2m)!}{s!(2m-2s)!}\\&\times\left(\mathrm{i}w_x\Big/\sqrt{\left(\frac{Q_x^2}{4}\right)^2-\frac{Q_x^2}{4}w_x^2}\right)^{2m-2s}\left((2m-2s)p^{2m-2s-1}-\frac{2p^{2m-2s+1}}{Q_x^2}\right)\\&\times\sum_{n=0}^{N}b_{2n}\left(1-\frac{4w_y^2}{Q_y^2}\right)^n H_{2n}\left(\frac{1}{2}\mathrm{i}w_y q\Big/\sqrt{\left(\frac{Q_y^2}{4}\right)^2-\frac{Q_y^2}{4}w_y^2}\right),\end{aligned} \tag{17b}$$

$$A_{oy}(p,q;z) = -\frac{1}{k_0^2 n_o^2}\frac{\pi f_x f_y}{2w_x w_y}\frac{1}{P_x}\frac{1}{P_y}\exp\left(-\frac{p^2}{P_x^2}\right) \times \exp\left(-\frac{q^2}{P_y^2}\right)\sum_{m=0}^{N} a_{2m}\left(1-\frac{4w_x^2}{P_x^2}\right)^m \sum_{s=0}^{m}(-1)^s \frac{(2m)!}{s!(2m-2s)!} \times \left(\mathrm{i}w_x \Big/ \sqrt{\left(\frac{P_x^2}{4}\right)^2 - \frac{P_x^2}{4}w_x^2}\right)^{2m-2s} \left((2m-2s)p^{2m-2s-1} - \frac{2p^{2m-2s+1}}{P_x^2}\right) \times \sum_{n=0}^{N} b_{2n}\left(1-\frac{4w_y^2}{P_y^2}\right)^n \sum_{t=0}^{n}(-1)^t \frac{(2n)!}{t!(2n-2t)!}\left(\mathrm{i}w_y \Big/ \sqrt{\left(\frac{P_y^2}{4}\right)^2 - \frac{P_y^2}{4}w_y^2}\right)^{2n-2t} \times \left((2n-2t)q^{2n-2t-1} - \frac{2q^{2n-2t+1}}{P_y^2}\right). \quad (17c)$$

By using Eqs. (17a) and (17c), the electric field component E_y of the light inside the uniaxial crystals can be obtained:

$$E_y(p,q;z) = \exp(ik_0 n_e z)A_{ey}(p,q;z) + \exp(ik_0 n_o z)A_{oy}(p,q;z). \quad (18)$$

Equations (13), (17) and (18) are the main analytical results of this paper, which provide a flexible approach to study diffraction properties of a Lorentz-Gauss beam at an arbitrary distance z in uniaxial crystals orthogonal to the optical axis. Based on the analytical expressions derived above, diffraction fields and intensity distributions of Lorentz-Gauss beams in uniaxial crystals can be investigated by detailed numerical examples.

3 Numerical results

In this section, based on Eqs. (13), (17) and (18), some numerical examples are illustrated to show the diffraction properties of Lorentz-Gauss beams in a rutile crystal orthogonal to the optical axis. In this paper the uniform calculation parameters in all figures are $\lambda = 632.8$ nm, $w_0 = 20$ μm, $n_o = 2.616$, $n_e = 2.903$, unless otherwise stated. It can be indexed from Refs. [12,28] that, $a_0 = 0.7399$, $a_2 = 0.9298\times10^{-2}$. When the even number $2m$ ($2n$) subsequently increases, both a_{2m} and b_{2n} dramatically decrease. Therefore, the expanded number N should not be large in computations. In this paper $N = 20$ is chosen for our numerical simulations, and Ref. [28] has proved that this approximate method is precise and convenient for computations.

Figure 1 shows the transversal field amplitude $|A_{ex}|$ (computed by Eq. (13)) of the extraordinary beam originated by the incident Lorentz-Gauss beam propagating in uniaxial crystals orthogonal to the optical axis, at several planes z. Beam parameters are $w_x = w_y = 20$ μm. From figures it can be found that $|A_{ex}|$ possess more side-lobes as z increases. When z subsequently increases, $|A_{ex}|$ would finally convert into a four-petal profile (see Fig. 1(d)).

Figure 2 describes the profile of transversal field amplitude $|E_y|$ (computed by Eq. (18)) of Lorentz-Gauss beams propagating in uniaxial crystals orthogonal to the optical axis, at several planes z. Beam parameters are the same as Fig. 1. From Fig. 2(a) it is indicated that, in the initial incident plane, $|E_y| = 0$. This phenomenon corresponds well to the analytical result by substituting $z = 0$ μm into Eq. (18), and it also corresponds well to illustrations of some previous reports [18,21]. When propagation distance increases, many lobes of beam profile begin to occur. In the far field region, $|E_y|$ would also convert into a four-petal profile, which is similar to that shown in Fig. 1(d).

Figure 3 represents the profile of longitudinal field amplitude $|A_{ez}|$ (computed by Eq. (17b)) of Lorentz-Gauss beams propagating in uniaxial crystals orthogonal to the optical axis, at several planes z. Beam parameters are the same as Fig. 1. From Fig. 3 we can find that, the longitudinal field component $|A_{ez}|$ in the initial incident plane has many lobes. However, when propagation distance z increases, distributions of these lobes would be destroyed and finally four-petal lobes start to emerge. Comparing Fig. 3 with Fig. 1 and Fig. 2, it is found that $|E_y| \ll |A_{ez}| \ll |A_{ex}|$ is satisfied, which corresponds well to some previous reports [18,21] describing diffraction properties of some other beams in uniaxial crystals.

Figure 4 shows the intensity distributions of Lorentz-Gauss beams propagating in uniaxial crystals orthogonal to the optical axis, at several reference planes z. Beam parameters are the same as Fig. 1. Comparing Fig. 4(a) to Fig. 1 of Ref. [8], it can be concluded that, when the Lorentz-Gauss beam propagates in anisotropic media, its intensity distribution would deteriorate and lose its initial

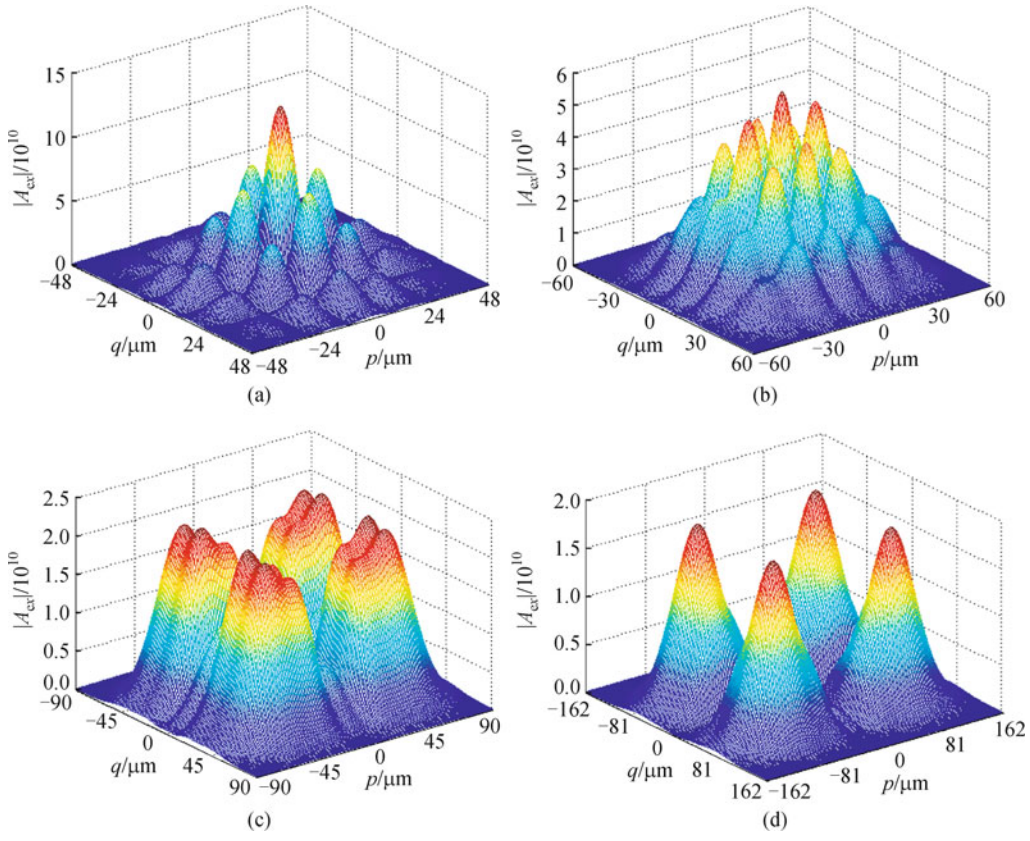


Fig. 1 Profiles of transversal fields $|A_{ex}|$ of Lorentz-Gauss beams propagating in uniaxial crystals at different planes. (a) z = 0 μm; (b) z = 2000 μm; (c) z = 5000 μm; (d) z = 10000 μm (beam parameters $w_x = w_y$ = 20 μm)

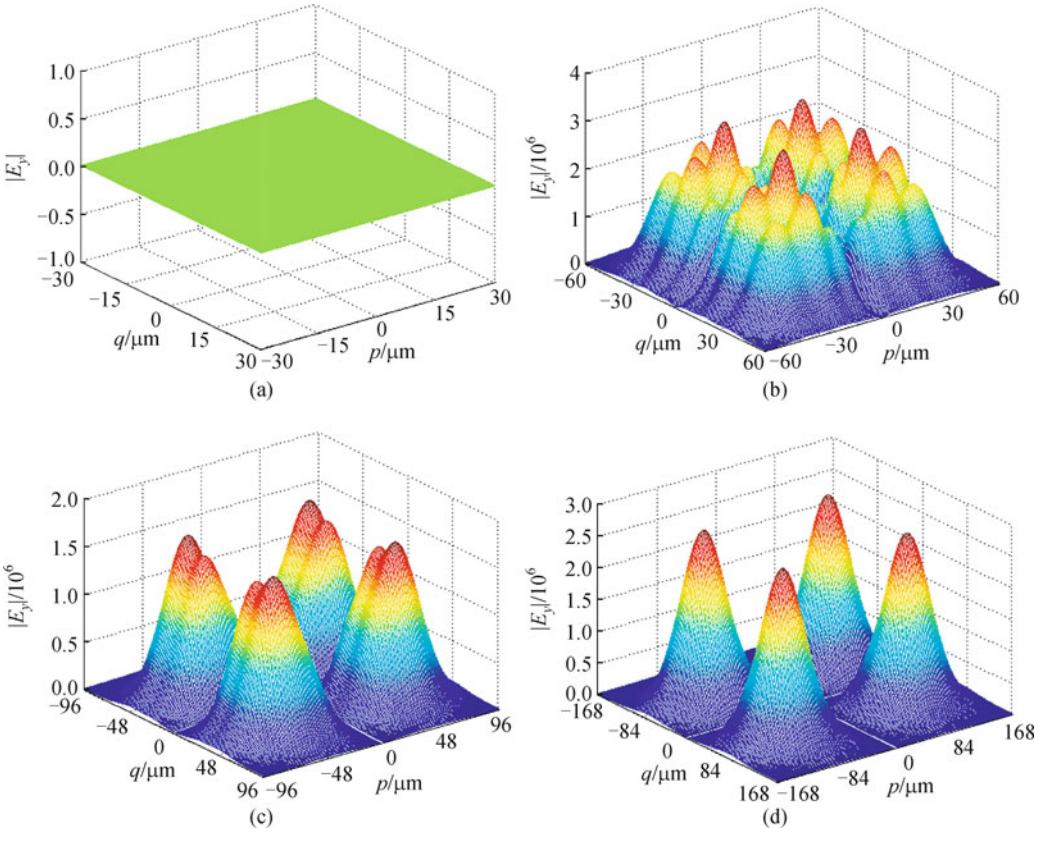


Fig. 2 Profiles of transversal fields $|E_y|$ of Lorentz-Gauss beams propagating in uniaxial crystals at different planes. (a) z = 0 μm; (b) z = 2000 μm; (c) z = 5000 μm; (d) z = 10000 μm (beam parameters are the same as Fig. 1)

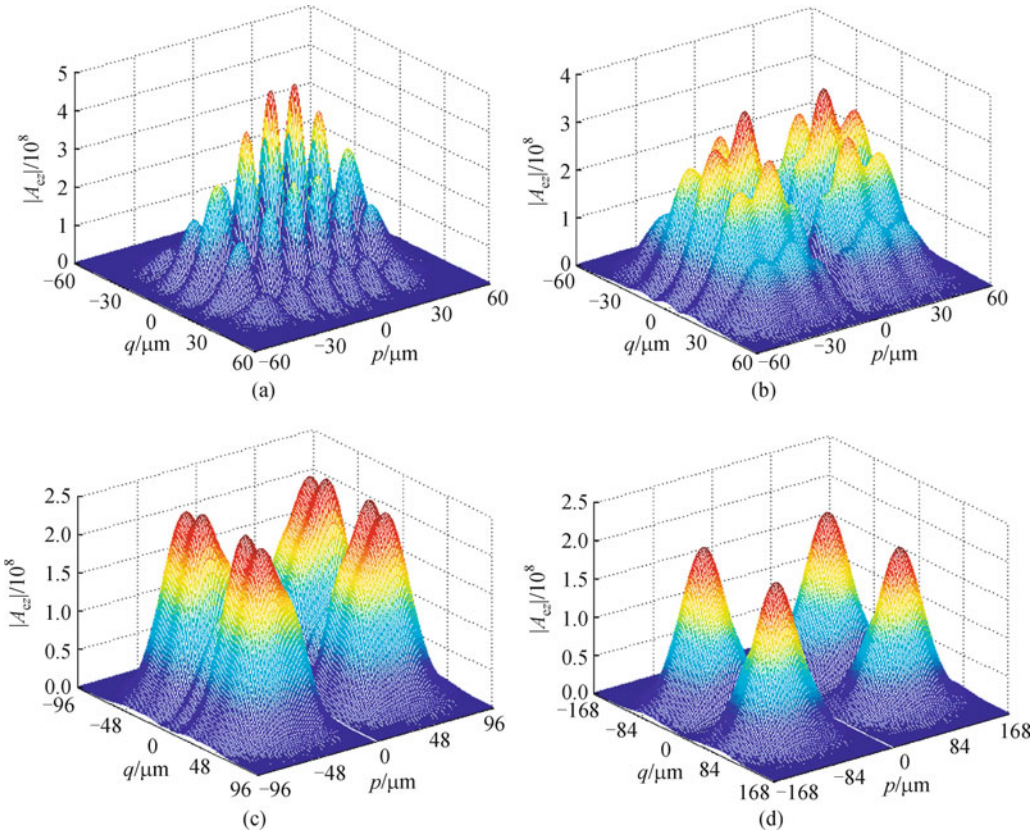


Fig. 3 Profiles of longitudinal fields $|A_{ez}|$ of Lorentz-Gauss beams propagating in uniaxial crystals at different planes. (a) z = 0 μm; (b) z = 2000 μm; (c) z = 5000 μm; (d) z = 10000 μm (beam parameters are the same as Fig. 1)

profile due to the different spreading speed in x and y directions. As a consequence, some side-lobes emerge because of the effect of the anisotropic media. When the propagation distance subsequently increases, more side-lobes begin to occur (see Fig. 4(b)). When the Lorentz-Gauss beam diffracts into the far field, its intensity distribution finally converts into a four-petal profile (see Fig. 4(d)). Numerical results also show that, when the propagation distance is even larger, this generated four-petal profile would preserve all along the propagation, which is not illustrated here to save space.

Figures 5 and 6 represent the normalized intensity distributions of Lorentz-Gauss beams with different values of w_x, w_y at planes z = 2000 μm and 5000 μm, respectively. From figures it can be observed that, beam parameters w_x and w_y have a strong influence on intensity distributions of Lorentz-Gauss beams in uniaxial crystals. For example, comparing Fig. 5(a) with Fig. 5(b), we can find that when w_y or w_x increases, the beam profile correspondingly changes. A similar phenomenon is illustrated in Fig. 6, for propagation distance z = 5000 μm. From these two figures, we can conclude that when w_x or w_y changes, the beam profile would loss its initial symmetric distribution upon propagating in uniaxial crystals.

One significant point that needs to be stressed is that, the analytical formulas (Eqs. (16) and (17)) are only the approximate format for the diffracted optical field of Lorentz-Gaussian beams. This is because, according to the deduction shown in Ref. [28], only if widths of the Lorentz parts w_x, w_y are sufficiently small, the expansion method is accurate. Also, observing from Fig. 1 of Ref. [28], one can deduce that, the larger is the expanded number N, the more accurate the approximate method applies. Therefore, the exact diffracted field of Lorentz-Gaussian beams is somewhat different from our approximated ones shown in Fig. 1 to Fig. 6. One reason of this difference is that, when the expanded approximation is made, a Gibbs-like phenomenon induced by the remaining oscillation in the wings appears but shown not to be serious for most applications (detailed origination see Fig. 1 of Ref. [28]). Another reason is the effect of the non-paraxial propagation. This is because, generally the Lorentz-Gauss beam is produced in double heterojunction $Ga_{1-x}Al_xAs$ laser resonators, so highly divergent optical fields are realizable in the far field of this beam. In this case the non-paraxial effect should also be considered in the exact diffracted field. So Eqs. (13), (17) and (18) in this paper can only provide an approximate description of the diffracted field.

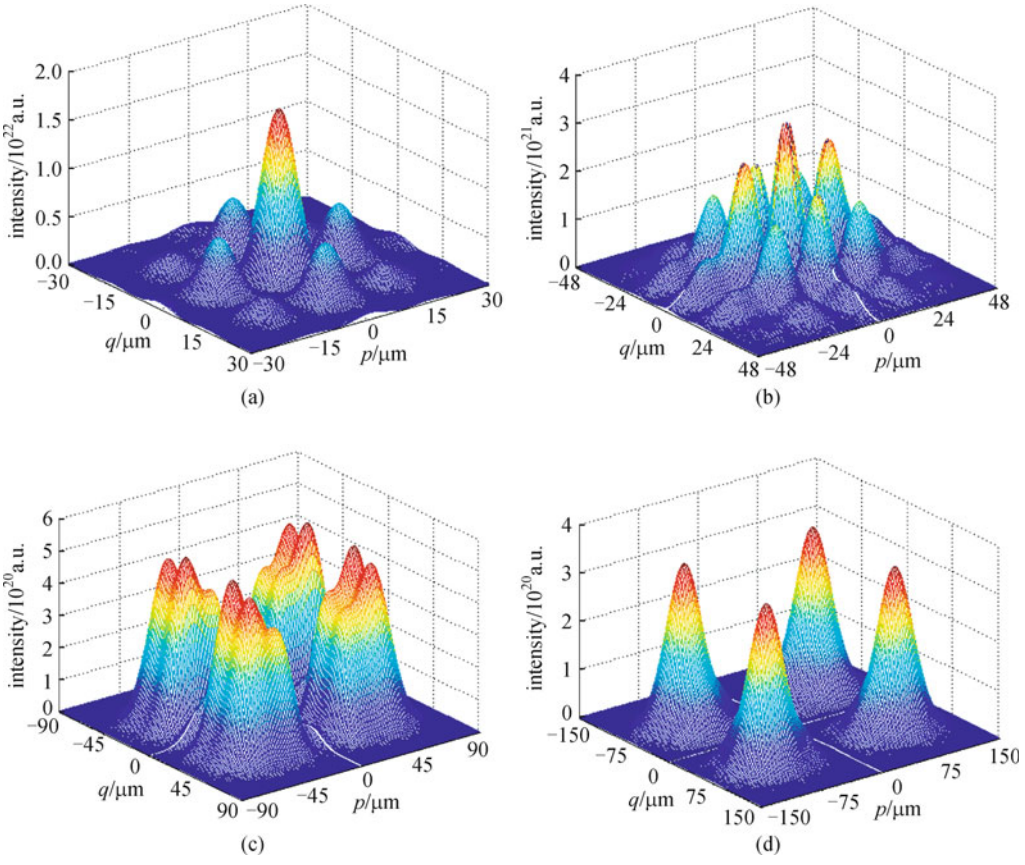


Fig. 4 Intensity distributions of Lorentz-Gauss beams propagating in uniaxial crystals at different planes. (a) z = 500 μm; (b) z = 2000 μm; (c) z = 5000 μm; (d) z = 10000 μm (beam parameters are the same as Fig. 1)

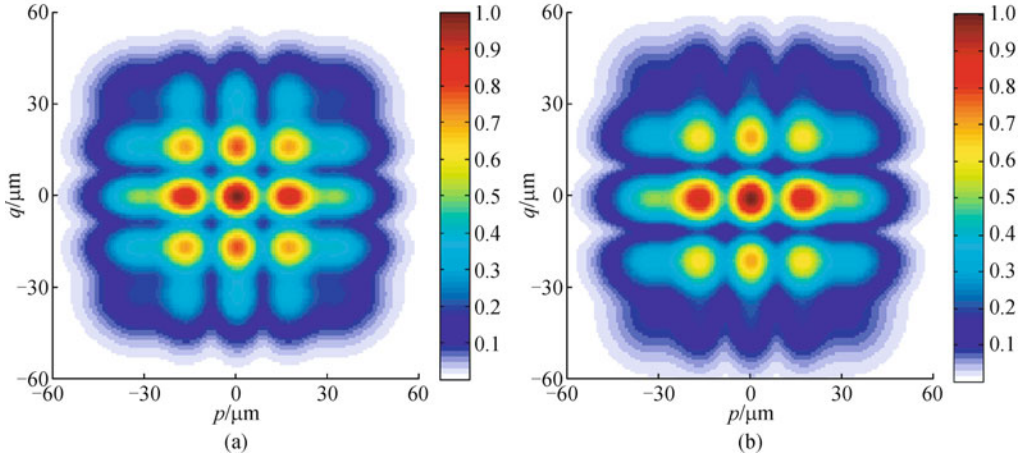


Fig. 5 Normalized intensity distributions of Lorentz-Gauss beams with different beam parameters propagating in uniaxial crystals at plane z = 2000 μm. (a) $w_x = w_y$ = 10 μm; (b) w_x = 10 μm, w_y = 20 μm

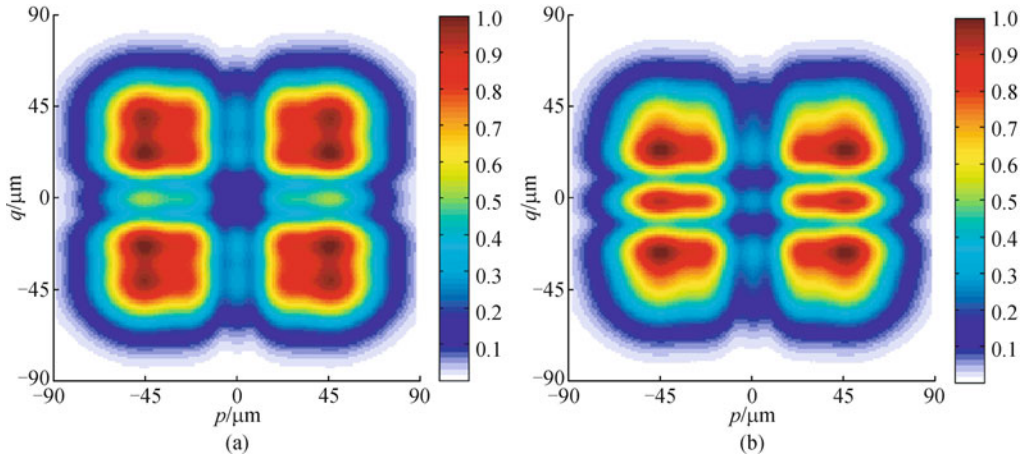


Fig. 6 Normalized intensity distributions of Lorentz-Gauss beams with different beam parameters propagating in uniaxial crystals at plane z = 5000 μm. (a) $w_x = w_y$ = 10 μm; (b) w_x = 10 μm, w_y = 20 μm

4 Conclusion

Based on the diffraction theory of beams in uniaxial crystals and analytical model expansions of beams, diffraction properties of Lorentz-Gauss beams in uniaxial crystals orthogonal to the optical axis are derived in analytical forms. Diffraction field components and intensity distributions of Lorentz-Gauss beams are investigated by detailed numerical examples. Effects of beam parameters w_x and w_y on intensity distributions are also studied. Obtained results show that diffraction field components and intensity distributions of Lorentz-Gauss beams would deteriorate upon propagation in uniaxial crystals, and this result is induced by the effect of anisotropic media. When the Lorentz-Gauss beam diffracts into the far field (z is large enough), its intensity distribution would finally convert into a four-petal profile. Beam parameters w_x and w_y also have a strong influence on intensity distributions of Lorentz-Gauss beams in uniaxial crystals. When w_x or w_y changes, beam profiles would lose their initial symmetry upon propagation.

Acknowledgements This work was supported by the National High Tech Research and Development Program of China (No. 2007AA04Z181), the NUST Research Funding (No. 2010ZYTS031) and the Excellent Doctorial Candidate Training Funding in NUST. The author is indebted to the reviewers for their valuable comments.

References

1. Casey H C, Panish M B. Heterostructure Lasers. New York: Academic Press, 1978
2. Dumke W P. The angular beam divergence in double-heterojunction lasers with very thin active regions. IEEE Journal of Quantum Electronics, 1975, QE-11(7): 400–402
3. Naqwi A, Durst F. Focusing of diode laser beams: a simple mathematical model. Applied Optics, 1990, 29(12): 1780–1785
4. Joyce W B, DeLoach B C. Alignment of Gaussian beams. Applied Optics, 1984, 23(23): 4187–4196
5. Gawhary O E, Severini S. Lorentz beams and symmetry properties in paraxial optics. Journal of Optics A: Pure and Applied Optics, 2006, 8(5): 409–414
6. Gawhary O E, Severini S. Lorentz beam as a basis for a new class of rectangular symmetric optical fields. Optics Communications, 2007, 269(2): 274–284
7. Yang J, Chen T, Ding G, Yuan X. Focusing of diode laser beams: a partially coherent Lorentz model. Proceedings of SPIE, 2007, 6824: 68240A
8. Zhou G. Nonparaxial propagation of a Lorentz-Gauss beam. Journal of the Optical Society of America B, 2009, 26(1): 141–147
9. Zhou G. Analytical vectorial structure of a Lorentz-Gauss beam in the far field. Applied Physics B: Lasers and Optics, 2008, 93(4): 891–899
10. Zhou G. Focal shift of focused truncated Lorentz-Gauss beam. Journal of the Optical Society of America A, 2008, 25(10): 2594–2599
11. Zhou G. Fractional Fourier transform of Lorentz-Gauss beams. Journal of the Optical Society of America A, 2009, 26(2): 350–355
12. Zhou G, Chu X. Average intensity and spreading of a Lorentz-Gauss beam in turbulent atmosphere. Optics Express, 2010, 18(2): 726–731
13. Zhou G. Propagation of a partially coherent Lorentz-Gauss beam through a paraxial ABCD optical system. Optics Express, 2010, 18 (5): 4637–4643
14. Born M, Wolf E. Principles of Optics. Oxford: Pergamon Press, 1999
15. Ciattoni A, Palma C. Optical propagation in uniaxial crystals orthogonal to the optical axis: paraxial theory and beyond. Journal of the Optical Society of America A, 2003, 20(11): 2163–2171
16. Ciattoni A, Palma C. Nondiffracting beams in uniaxial media propagating orthogonally to the optical axis. Optics Communications, 2003, 224(4–6): 175–183
17. Ciattoni A, Palma C. Anisotropic beam spreading in uniaxial

crystals. Optics Communications, 2004, 231(1–6): 79–92
18. Liu D, Zhou Z. Various dark hollow beams propagating in uniaxial crystals orthogonal to the optical axis. Journal of Optics A: Pure and Applied Optics, 2008, 10(9): 095005
19. Liu D, Zhou Z. Propagation of partially polarized, partially coherent beams in uniaxial crystals orthogonal to the optical axis. European Physical Journal D, 2009, 54(1): 95–101
20. Liu D, Zhou Z. Propagation of partially coherent flat-topped beams in uniaxial crystals orthogonal to the optical axis. Journal of the Optical Society of America A, 2009, 26(4): 924–930
21. Tang B. Hermite-cosine-Gaussian beams propagating in uniaxial crystals orthogonal to the optical axis. Journal of the Optical Society of America A, 2009, 26(12): 2480–2487
22. Ciattoni A, Cincotti G, Palma C. Ordinary and extraordinary beams characterization in uniaxially anisotropic crystals. Optics Communications, 2001, 195(1–4): 55–61
23. Ciattoni A, Crosignani B, Di Porto P. Vectorial theory of propagation in uniaxially anisotropic media. Journal of the Optical Society of America A, 2001, 18(7): 1656–1661
24. Ciattoni A, Cincotti G, Provenziani D, Palma C. Paraxial propagation along the optical axis of a uniaxial medium. Physical Review E, 2002, 66(3): 036614
25. Ciattoni A, Cincotti G, Palma C. Propagation of cylindrically symmetric fields in uniaxial crystals. Journal of the Optical Society of America A, 2002, 19(4): 792–796
26. Cincotti G, Ciattoni A, Palma C. Laguerre-Gauss and Bessel-Gauss beams in uniaxial crystals. Journal of the Optical Society of America A, 2002, 19(8): 1680–1688
27. Tang B, Jin Y, Jiang M, Jiang X. Diffraction properties of four-petal Gaussian beams in uniaxially anisotropic crystal. Chinese Optics Letters, 2008, 6(10): 779–781
28. Schmidt P P. A method for the convolution of lineshapes which involve the Lorentz distribution. Journal of Physics B, 1976, 9(13): 2331–2339
29. Abramowitz M, Stegun I A. Handbook of Mathematical Functions. New York: Dover Publication, 1972